International Journal of Aquatic Science
ISSN: 2008-8019
Vol 2, No 1, 2011

Motion characteristics of a Korean designed submersible fish cage system in waves and currents using numerical analysis

Tae-Ho Kim*

School of Marine Technology, Chonnam National University, Yeosu 550-749, Korea

Abstract

A numerical model analysis was performed to analyze the motion of a Korean designed automatic submersible fish cage system in waves and currents. The fish cage system consisted of a 12-angle rigid frame, net cage, cover net, 12 upper floats, 12 tanks (for fixed and variable ballast), mooring ropes, anchors, and control station. Simulations were performed with the cage at the surface of the water and at a depth of 20 m. Using a Morison equation type model, simulations of the system were conducted on the two configurations. The force parameters described both regular and random waves, with and without currents, and their values were considered as input to the model. Heave, surge and pitch dynamic calculations were made. Results were analyzed in both the time and frequency domains and where appropriate, linear transfer functions were calculated.

Key Word: Numerical model, Submerging and surfacing, Morison equation, Linear transfer function.

Introduction:

In Korea, the high concentration of marine aquaculture facilities in the inner bays has led to ecological and environmental problems along the shore. In recent years, operations have gradually been moved from the sheltered inshore waters to more exposed sites, where higher growth rates of fish are expected, because of better water quality. Most of the existing fish cage systems, however, utilize net cages mounted to raft-type structures, which maintain buoyancy with styrofoam mounted under a wooden square collar. These cage systems are fragile and can be damaged by typhoons, high waves, and strong currents. These

(✉) kimth@chonnam.ac.kr

systems are typically not suitable for exposed, offshore sites. To continue high-quality fish production at exposed sites, a new fish cage system that can be operated safely in high waves or strong currents needed to be developed (Kim et al., 2010a).

For the reduction of the wave and current loadings on a fish cage system, a submersible fish cage system was developed. For example, several offshore submersible cages such as PolarCirkle, SUBflex, SADCO Shelf and Ocean Spar, which are operated by compressed air, have been recently developed (Mitrovich, 2010). In particular, several submersible Ocean Spar fish cages (from the United States) have recently been deployed off the Jeju islands in Korea. Experience has shown that these systems require two or more divers for proper maintenance, which incurs substantial expenses. Similar to the traditional Korean surface cages, that allow harvesting, stock inventory and inspection without the need for divers, a new system was needed to be developed to save operational costs. Thus, a submersible fish cage system which can move vertically within the water column through adjustments of the weight and buoyancy of the cage with an automatic control system has been developed. The performances of the cage system were reported by Kim et al. (2010b).

A numerical model study was conducted to investigate the motion of an automatic submersible cage system. The system was analyzed using a spread mooring configuration with four anchor legs. The numerical model used the Finite Element Analysis approach described in Tsukrov et al. (2003 and 2005). The results of past model simulations were in good agreement with the results of both physical model tests and field measurements for a variety of cage/mooring configurations and conditions (DeCew et al., 2005; Fredriksson et al., 2003a, 2003b; Kim 2006; Kim et al., 2008). Though the results of the model should only be considered as approximate, an insight into the motion response of the fish containment structure was gained.

The objectives of this study were to determine the motion response of the cage system at two locations within the water column. A numerical model was constructed, simulations were performed and responses were obtained.

Materials and methods:

1. Structure of submersible fish cage system

The automatic control system of the fish cage monitors environmental parameters such as wave height and wind speed so the cage can be submerged in extreme sea states and then surfaced after the weather passed (Kim et al., 2010). Being able to remotely remove fish cages from the sea surface during extreme storm events will help to prevent damage. The fish cage system consisted of a 12-angle rigid frame,

net cage, cover net, 12 upper floats, 12 tanks (for fixed and variable ballast), mooring ropes, anchors, and control station, as shown in Fig. 1. In particular, the upper part of the frame contained fixed flotation and the lower part with both fixed ballast tanks and variable ballast tanks. The buoyancy of the variable ballast tanks was remotely adjustable. A surface control system operates a switch that enables gas (such as nitrogen or air) or seawater to enter the tanks to either submerge or surface the fish cage. The control station can regulate both the inflow and outflow of gas or seawater to and from the variable ballast tanks in response to the surface environmental conditions. The control station incorporates wave and wind speed sensors, with a GPS, and an A/D-D/A board along with data acquisition components and software. The cage is fixed to the bottom using a spread mooring system. The cage can move vertically through the water column by a single grid square connected to the mooring system. The details of the cage system are shown in Tab. 1.

2. Numerical Model

Numerical model simulations were performed using a finite element computer program developed specifically for marine aquaculture applications. The program was described in Tsukrov et al. (2003) and (2005). Wave and current loadings on truss and buoy elements were introduced to the model simulations by utilizing the Morison equation (Morison et al, 1950). The algorithm employed a nonlinear Lagrangian formulation to account for large displacements of structural elements. In addition, the unconditionally stable Newmark direct integration scheme was adopted to solve the nonlinear equations of motion. Hydrodynamic forces on the structural elements were calculated using the Morison equation modified to account for relative motion between the structural element and the surrounding fluid as described by Haritos and He (1992).

The nets of the aquaculture cage were modeled with special considerations. A "net element" that was constructed to reproduce the drag, buoyancy, inertial and elastic forces exerted on the structure by currents and waves was used. A modeling technique was developed, called the "Consistent Net Element", that considered these important forces, since direct finite element modeling of all the strands was impractical. The detailed approach was described explicitly in Tsukrov et al. (2003).

The numerical model required all of the geometric and material properties of the fish cage was prescribed. The parameters included the mass density, Young's modulus and cross sectional area of each element component. Based on the information provided in Tab. 1, the models of the components were determined according to the results provided in Tab. 2.

Along with the material and geometric properties, the dimensions and configuration of the submersible fish cage system were then used to design the numerical model. Schematic model is shown in Fig. 2. Also shown in Fig. 2 is the orientation of the system to the wave and current loading.

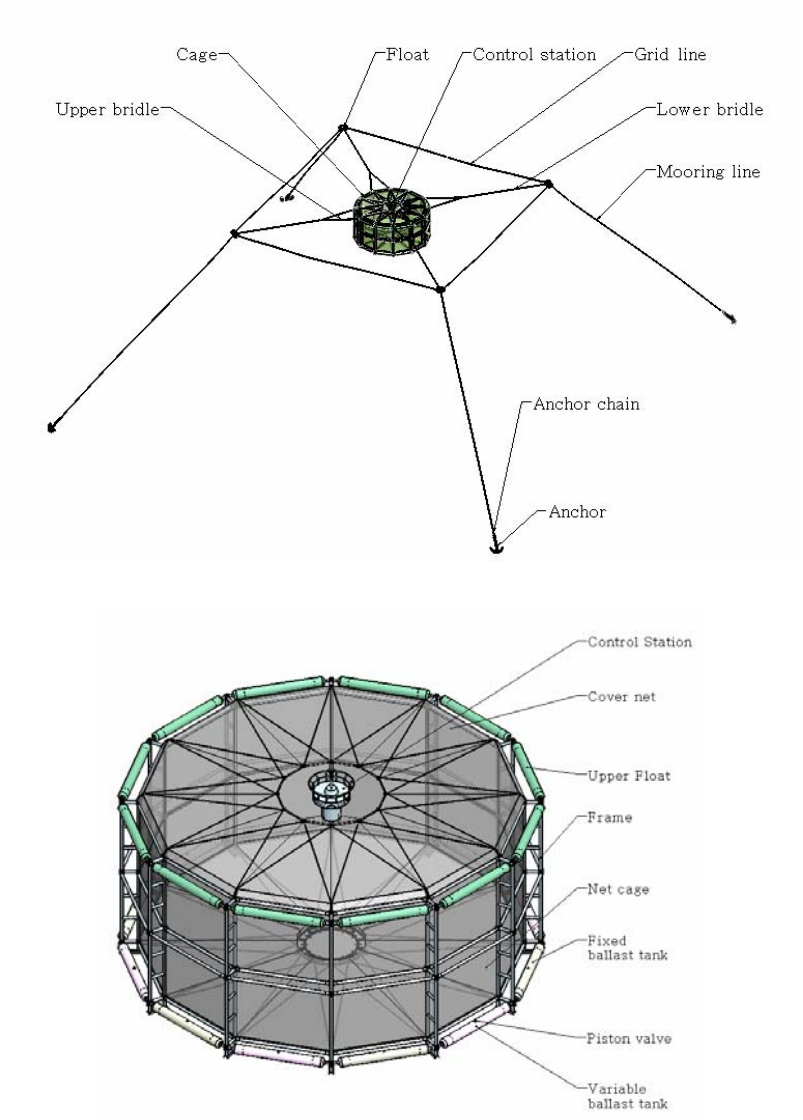

Figure 1: General schematic plan of a Korean automatic submersible fish cage system with a spread mooring system.

Table 1: Details of a Korean automatic submersible fish cage system.

Component	Parameter	Value
Upper floats	Material	Steel
	Diameter	560 mm
	Overall length	6240 mm
Fixed floats	Material	Steel
	Diameter	560 mm
	Overall length	6240 mm
Variable floats	Material	Steel
	Diameter	560 mm
	Overall length	6240 mm
Frame	Material	Steel
	Diameter	150 mm
Inner frame	Material	Steel
	Diameter	150 mm
Inner ring	Material	Steel
	Overall diameter	150 mm
Net	Material	Dyneema
	Twine diameter	2.2 mm
	Bar length	60 mm
Support line	Material	Dyneema
	Diameter	22 mm

Table 2: Details of a Korean submersible fish cage component model.

Component	Parameter	Value
Upper floats	Density	235.2 kg/m^3
	Modulus of elasticity	2.0 x 10^{11} Pa
	Cross sectional area	0.209 m^2
Fixed floats	Density	1025 kg/m^3
	Modulus of elasticity	2.0 x 10^{11} Pa
	Cross sectional area	0.209 m^2
Variable floats	Density (surface cage)	1481 kg/m^3
	Density (submerged cage)	1579 kg/m^3
	Modulus of elasticity	2.0 x 10^{11} Pa
	Cross sectional area	0.209 m^2
Frame	Density	1638 kg/m^3
	Modulus of elasticity	2.0 x 10^{11} Pa
	Cross sectional area	0.0202 m^2
Inner frame	Density	1534 kg/m^3
	Modulus of elasticity	2.0 x 10^{11} Pa
	Cross sectional area	0.0209 m^2
Inner ring	Density	2559 kg/m^3
	Modulus of elasticity	2.0 x 10^{11} Pa
	Cross sectional area	0.012 m^2
Net	Density	994 kg/m^3
	Modulus of elasticity	1.02x 10^{11} Pa
	Cross sectional area	3.801 x 10^{-6} m^2
Stiffener	Density	1025 kg/m^3
	Modulus of elasticity	2.5 x 10^{11} Pa
	Cross sectional area	5.00 x 10^{-6} m^2
Support line	Density	994 kg/m^3
	Modulus of elasticity	1.02 x 10^{11} Pa
	Cross sectional area	3.801 x 10^{-4} m^2

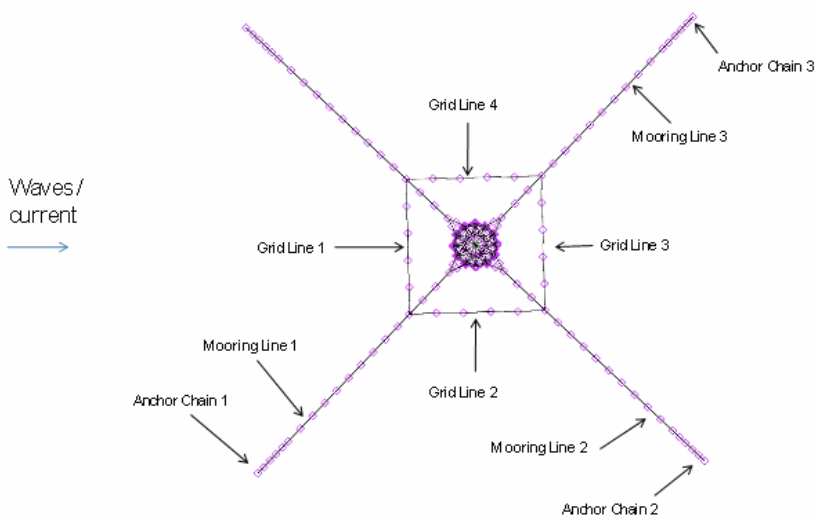

Figure 2: Overview of the numerical model system components.

Simulations were performed with the cage at the surface and at a depth of 20 m, as shown in Fig. 3. In both situations, the depth at the site was 50 m.

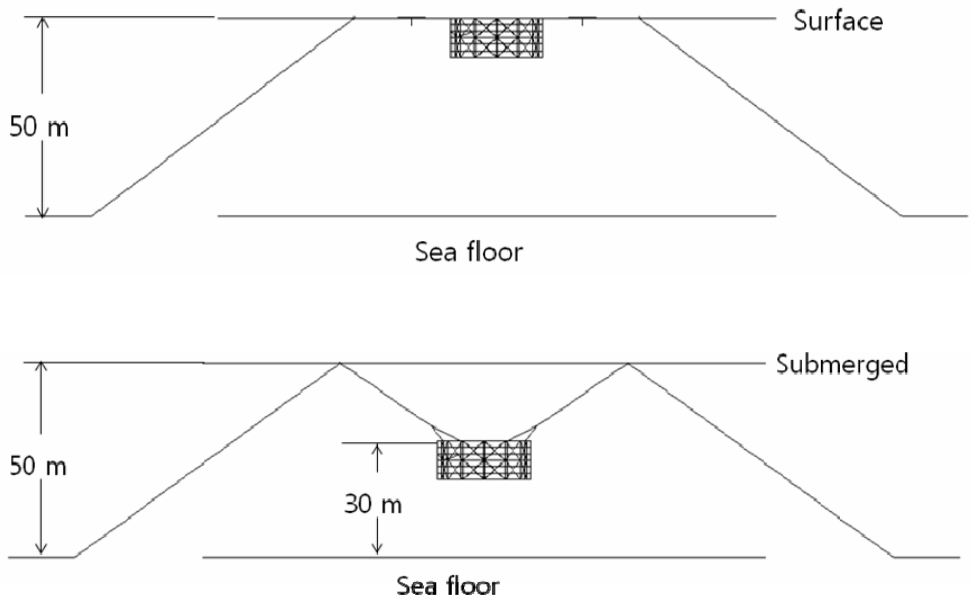

Figure 3: Side view of the fish cage at the surface and submerged positions.

3. Wave and current input parameters

The numerical model also required environmental forcing parameters. The first set of simulations was conducted with no wave and current load to verify static conditions. Once the static conditions were verified, forcing load consisting of regular and random wave conditions both with and without a superimposed current of 1.0 m/s were considered as input to the model. Twelve regular wave load cases were prescribed with and without current. The details are provided in Tab. 3. In addition to the regular wave, random wave simulations were also performed. The model was forced with a JONSWAP (Joint North Sea Wave Project) type wave profile with a significant wave height of 9.51 m and a peak period of 14.01 s, which were chosen according to a design wave condition of the southern sea in Korea for 20-year return periods (www.kordi.re.kr). For both the surface and submerged configurations, a total of 30 numerical model simulations were performed.

Table 3: Wave and current parameters for each regular wave load case.

Load case	Currents (m/s)	Wave height (m)	Period (s)
1	0	2.55	6.11
2	1.0	2.55	6.11
3	0	3.53	7.08
4	1.0	3.53	7.08
5	0	4.22	8.75
6	1.0	4.22	8.75
7	0	6.85	11.82
8	1.0	6.85	11.82
9	0	8.66	13.26
10	1.0	8.66	13.26
11	0	10.25	15.11
12	1.0	10.25	15.11

4. Cage motion response locations

For each simulation, motion response data sets were acquired to characterize the motion of the cage. The node locations chosen are shown in Fig. 4. The heave RAO (response amplitude operator) was calculated as the average vertical motion of the two rim nodes. The surge RAO was calculated as the average horizontal motion of the two rim nodes. The pitch RAO was calculated as the angle between the two upper rim nodes. Numerical model representations of the fish cage system are shown in Fig. 5.

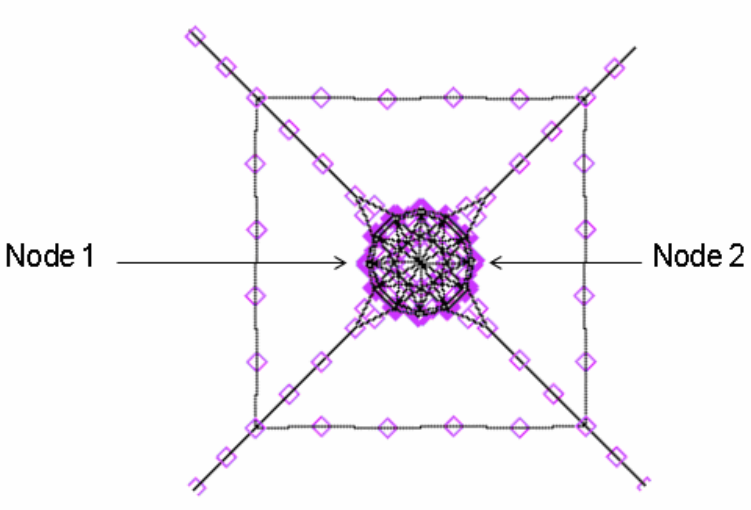

Figure 4: Node locations at which motion response data sets were obtained from the numerical model.

5. Data processing

1) Regular waves

Regular wave tests were conducted using numerical modeling methods for the load cases are indicated in Tab. 3. The characteristics of these waves were approximated using linear wave theory characterized by the following velocity potential (ϕ),

$$\phi = -A\frac{g}{2\pi f}\frac{\cosh k(d+z)}{\cosh kd}\sin(kx-2\pi ft), \quad (1)$$

surface elevation (η),

$$\eta = A\cos(kx-2\pi ft), \quad (2)$$

and dispersion relation,

$$(2\pi f)^2 = gk\tanh(kd), \quad (3)$$

where A is the wave amplitude (equal to ½ of the wave height), g is the gravitational constant, f is the frequency, k is the wave number equal to 2π/L, L is the wave length, d is the water depth, z is the vertical position in the water column and x is the horizontal position.

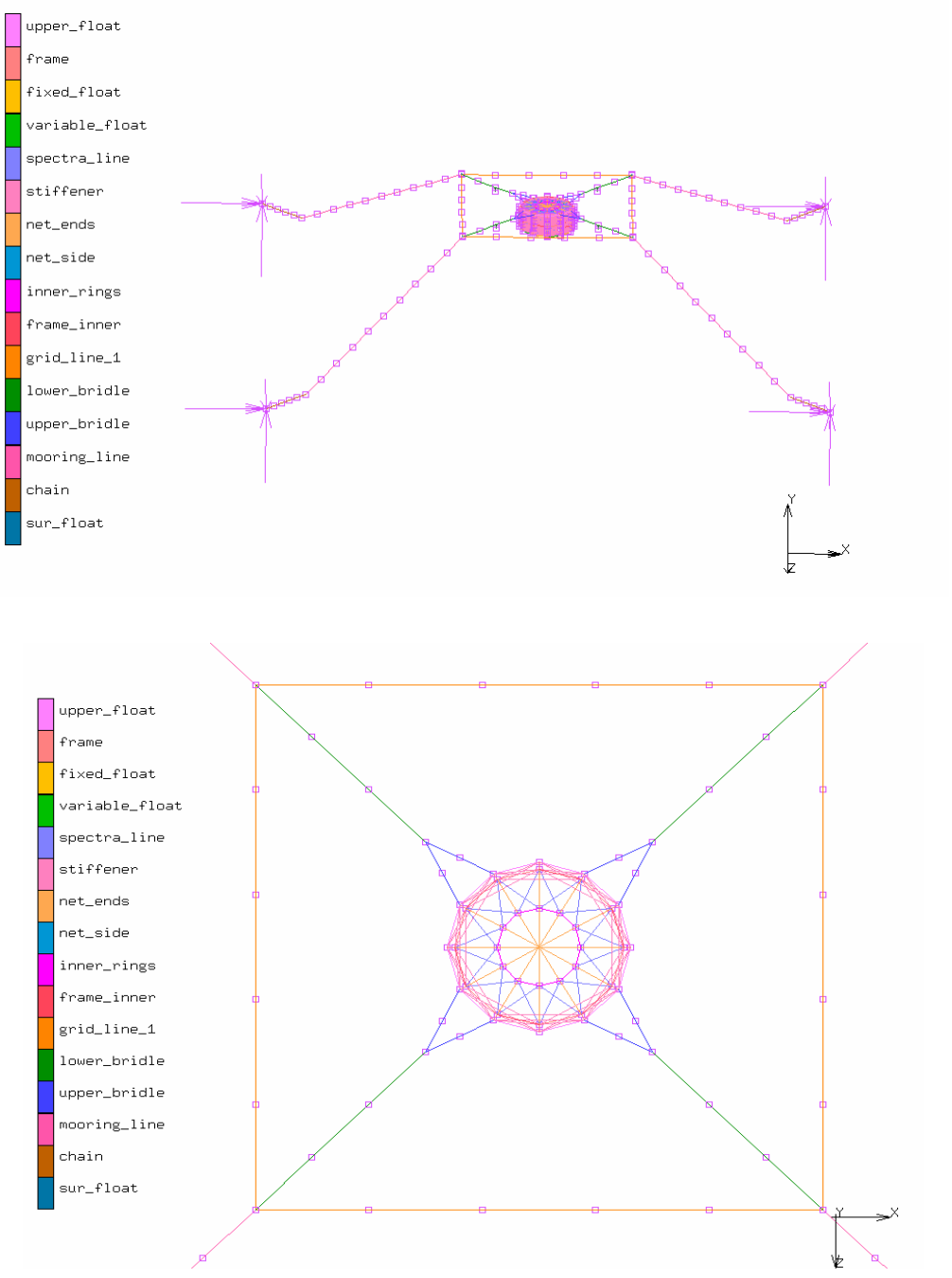

Figure 5: Numerical model representation of the fish cage system.

Linear transfer function magnitudes calculated for deterministic waves, referred to as response amplitude operators (RAOs), were obtained by dividing the amplitude of the response by the amplitude of the force for each wave frequency. The heave, surge and pitch RAOs are defined as,

- Heave RAO: heave amplitude/wave

elevation amplitude,

- Surge RAO: surge amplitude/wave excursion amplitude and
- Pitch RAO: pitch amplitude/wave slope amplitude.

The wave excursion amplitude (ζ) is defined as the horizontal semi-axis of the ellipse formed by the water particle trajectory (at the surface). It is found by taking the partial derivative of equation (1) with respect to x to obtain the horizontal velocity component. Integrating this result with respect to time (t), and dropping the oscillating term, gives the wave excursion amplitude

$$\zeta = A\frac{\cosh kd}{\sinh kd}. \quad (4)$$

The wave slope amplitude (θ) was obtained by taking the partial derivative of equation (2) with respect to x and dropping the oscillating term,

$$\theta = kA. \quad (5)$$

It should be noted that these processing techniques work well for the simulations with only waves since the response can be assumed to be linear. In the cases with a strong 1.0 m/s current, large movements can be considered as a high nonlinear response; therefore, the results of these analysis techniques were difficult to interpret. For this reason, the RAO calculations were carried out for load cases without the 1.0 m/s current.

2) Random waves

Force input to the numerical model also consisted of an irregular wave profile. To obtain an irregular wave profile in the numerical routine, a spectrum was decomposed into multiple frequency components. The spectrum selected was a form of the Joint North Sea Wave Project (JONSWAP) spectrum (Hasselman et al., 1973 and Goda, 2000) described by

$$S(f) = \alpha H_s^2 T_p^{-4} f^{-5} \exp\left[-1.25(T_p f)^{-4}\right]\gamma^Y, \quad (6)$$

where

$$Y = e^{\left[-(T_p f - 1)^2 / 2\sigma^2\right]},$$

$$\alpha = \frac{0.0624}{0.23 + 0.0336\gamma - 0.185(1.9+\gamma)^{-1}},$$

and

$$\sigma = \begin{cases} \sigma_a : f \le f_p \\ \sigma_b : f \ge f_p \end{cases},$$

and f_p is the frequency at the spectral peak ($1/T_p$). Parameters γ and σ were used to adjust the height and width of the peak of the curve, respectively. In this study, the default shaping parameters were used and are shown in Tab. 4, along with H_s of 9.51 m and T_p of 14.01 s.

Table 4: JONSWAP parameters used to shape the input spectrum.

Parameter	Value
H_s (m)	9.51
T_p (s)	14.01
γ	3.3
Power of f	-5
σ_a	0.07
σ_b	0.09

In this study, irregular waves (and the system response) were described by a spectrum in the frequency domain in terms of units proportional to energy per frequency band. The wave elevation auto-spectrum was typically described by the significant wave height and the dominant wave period. Statistically, the significant wave height was often estimated from the H_{mo} and calculated from the zeroth moment of the spectrum,

$$m_j = \int_0^\infty f^j G(f) df, \quad where\ j = 0 \ldots n, \text{ (7)}$$

where j=0 and G (f) is the one sided wave elevation auto-spectral density. The zeroth moment of the spectrum is also the area under the spectral curve equal to the variance. If the spectrum is narrow banded and the wave heights follow a Rayleigh probability distribution (Ochi, 1998), H_{mo} is obtained from,

$$H_{mo} = 4\sqrt{m_o}\ . \text{ (8)}$$

In deep water, H_{mo} is approximately equal to the average of the top third wave heights (Shore Protection Manual, 1984), which is the significant wave height (H_s) used in the JONSWAP spectrum. The dominant wave period, T_p, is one over the frequency at which the maximum energy in a spectrum occurs.

The wave elevation auto-spectrum was calculated from the measured times series using a discrete form of

$$S_{xx}(f) = \lim_{T \to \infty} \frac{1}{2T} X(f) X^*(f), \text{ (9)}$$

where S_{xx}(f) is the two sided, auto-spectral density function, $X^*(f)$ is the complex conjugate of $X(f)$ and T is the record length. The two sided auto-spectral density function is continuous for all frequencies between -∞ and ∞. In standard obser-vational practice, however, the one sided auto-spectral density function, $G_{xx}(f)$, is used, where

$$G_{xx}(f) = 2S_{xx}(f) \qquad 0 \le f \le \infty, \text{ (10)}$$

Note that G_{xx} (f) could be the same term used in equation (2). For the irregular wave tests, linear transfer functions were calculated as a function of frequency using auto- and cross-spectral methods. In the frequency domain, the system force can be described in terms of energy density as

$G_{\eta\eta}(f)$: Wave elevation auto-spectrum (m^2/Hz),

$G_{\zeta\zeta}(f)$: Wave excursion auto-spectrum (m^2/Hz) and

$G_{\theta\theta}(f)$: Wave slope auto-spectrum (rad^2/Hz).

The wave excursion and slope auto-spectra were calculated from the wave elevation auto-spectrum using the following relationships,

$$G_{\zeta\zeta}(f)=G_{\eta\eta}(f)\cdot[tanh(kd)]^{-2}, \quad (11)$$

and

$$G_{\theta\theta}(f)=G_{\eta\eta}(f)\cdot(k)^2, \quad (12)$$

respectively, where k=k(f) according to the dispersion relation.

Likewise, the auto-spectral motion resp-onse in heave, surge and pitch were calculated using

$G_{hh}(f)$: Heave response auto-spectrum (m^2/Hz),

$G_{ss}(f)$: Surge response auto-spectrum (m^2/Hz) and

$G_{pp}(f)$: Pitch response auto-spectrum (rad^2/Hz).

To obtain the linear transfer function using the auto-spectral technique between the force and the response, the following calculations were made,

$$|H_{hh}(f)|=\left[\frac{G_{hh}(f)}{G_{\eta\eta}(f)}\right]^{\frac{1}{2}}, \quad (13)$$

$$|H_{ss}(f)|=\left[\frac{G_{ss}(f)}{G_{\zeta\zeta}(f)}\right]^{\frac{1}{2}}, \quad (14)$$

$$|H_{pp}(f)|=\left[\frac{G_{pp}(f)}{G_{\theta\theta}(f)}\right]^{\frac{1}{2}}, \quad (15)$$

where $H_{hh}(f)$ is the heave transfer function, $H_{ss}(f)$ is the surge transfer function and $H_{pp}(f)$ is the pitch transfer function.

Like the regular waves, these processing techniques worked well for the simulations with only waves, since the response can be assumed to be linear.

Results and discussion:

The first set of numerical model simulations were performed without current and wave loading. In each of the simulations, the buoyancy of the cage moved the cage vertically as the mooring lines stretched, pre-tensioning the components. Two static simulations were performed. In the first simulation, the cage was placed at the surface where the depth of the rim was set at 0 m. In the second simulation, the cage was placed at a depth of 20 m. The static

data sets shown on Fig. 6 indicate the final heave, surge and pitch positions.

The next set of simulations was performed with regular waves with and without a 1.0 m/s current (co-linear) for the surface and submerged models. The wave and current parameters are shown on Tab. 3. The wave length (L), excursion (ζ) and the wave slope (θ) as calculated with equations (3), (4) and (5), respectively, are indicated on Tab. 5. Knowing the wave length, the wave number (k) can be calculated as 2π/L. The wave number for each of the simulations is also shown in Tab. 5.

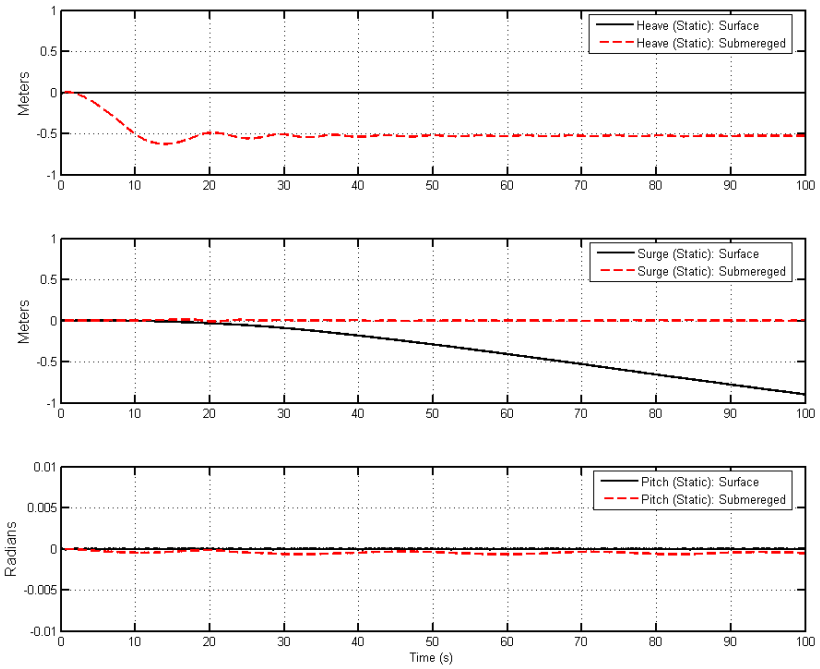

Figure 6: Motion results of the static simulations. Note that at time = 0 s, the cage is at its initial prescribed depth (surface: 0 m, submerged: 20 m).

Table 5: Calculated wave particulars for each load case.

Load case	A (m)	L (m)	k (rad/m)	ζ (m)	θ (rad)
1, 2	1.2750	58.2870	0.1078	1.2751	0.0845
3, 4	1.7650	78.2198	0.0803	1.7661	0.0455
5, 6	2.1100	118.3716	0.0531	2.1310	0.0252
7, 8	3.4250	200.0661	0.0314	3.7347	0.0092
9, 10	4.3300	237.9838	0.0264	4.9954	0.0061
11, 12	5.1250	285.4565	0.0220	6.4007	0.0043

A total of 24 simulations were conducted. Data sets were obtained for the motion of the fish cage in heave, surge and pitch. Examples of the resulting time series data sets are shown in Figs. 7 and 8 for the simulations with and without current, respectively. It should be noted that for all submerged cage simulations with current, the front lower rim of the cage touches the seafloor. Thus, when designing a full-scale fish cage system, countermeasures considering the buoyancy increase of the upper floats were needed to protect the situation. The comparison of times series data sets in Figs. 7 and 8 shows that the cage did move vertically in response to waves. Therefore, RAO calculations were only done for the cases without current (load cases 1, 3, 5, 7, 9 and 11). Heave, surge and pitch RAO values were obtained with equations (4) and (5) with the appropriate values from Tab. 6. The pitch motion was prominent for surface and submerged conditions. The heave motions, seriously affect the stability of a cage system, submerged below 20 m of the mean water line that were 52.35% to 86.02% smaller than those at the surface condition.

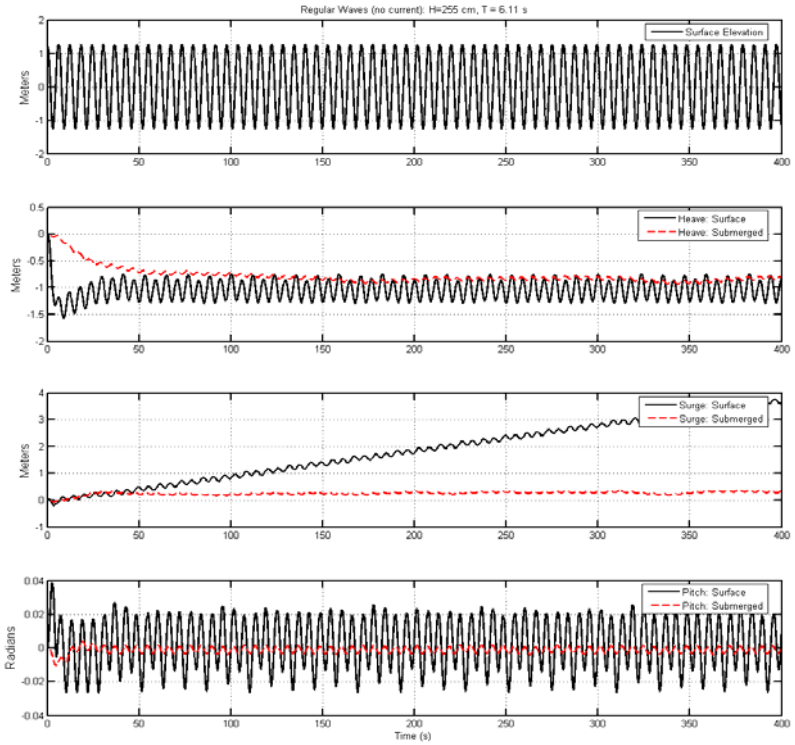

Figure 7: Motion time series results for the cage in both the surface and submerged positions with wave height of 2.55 m, period of 6.11 s and no current.

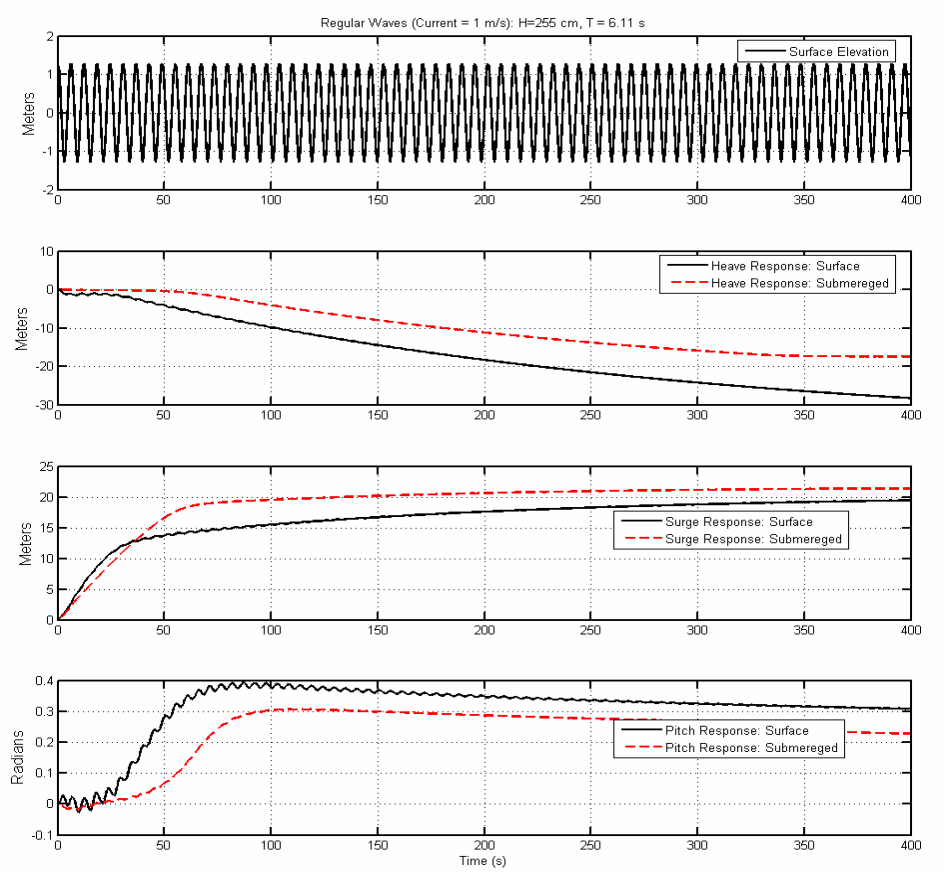

Figure 8: Motion time series results for the cage in both the surface and submerged positions with a wave height of 2.55 m, period of 6.11 s and with a 1.0 m/s current.

Table 6: Motion RAO values for the simulations without current.

Load case	Heave (m/m)		Surge (m/m)		Pitch (rad/rad)	
	Surface	Submerged	Surface	Submerged	Surface	Submerged
1	0.1831	0.0256	0.0663	0.0246	0.2416	0.0275
3	0.2458	0.0491	0.1363	0.0124	0.5499	0.1030
5	0.3241	0.1055	0.2418	0.0705	0.8669	0.2274
7	0.3825	0.0980	0.3452	0.0816	2.2109	0.8994
9	0.3849	0.1740	0.3683	0.2585	3.4571	0.8953
11	0.3893	0.1820	0.3879	0.3071	5.4865	2.2606

Once the static and regular wave tests were completed, the random wave tests were conducted with and without the 1.0 m/s superimposed current for both the surface and submerged configurations. Simulations were performed using the JONSWAP wave spectrum with and without the superimposed, co-linear current.

Using the time series results, the spectral representation of the wave input, motion response in heave, surge and pitch were calculated. The calculations were performed with the appropriate form of equation (10) to obtain the wave elevation ($G_{\eta\eta}$), heave (G_{hh}), surge (G_{ss}) and pitch (G_{pp}) response spectra. The input wave spectrum was used with equations (11) and (12) to calculate the wave excursion ($G_{\zeta\zeta}$) and wave slope ($G_{\theta\theta}$) spectra. Plots of each spectral result are indicated in Fig. 9.

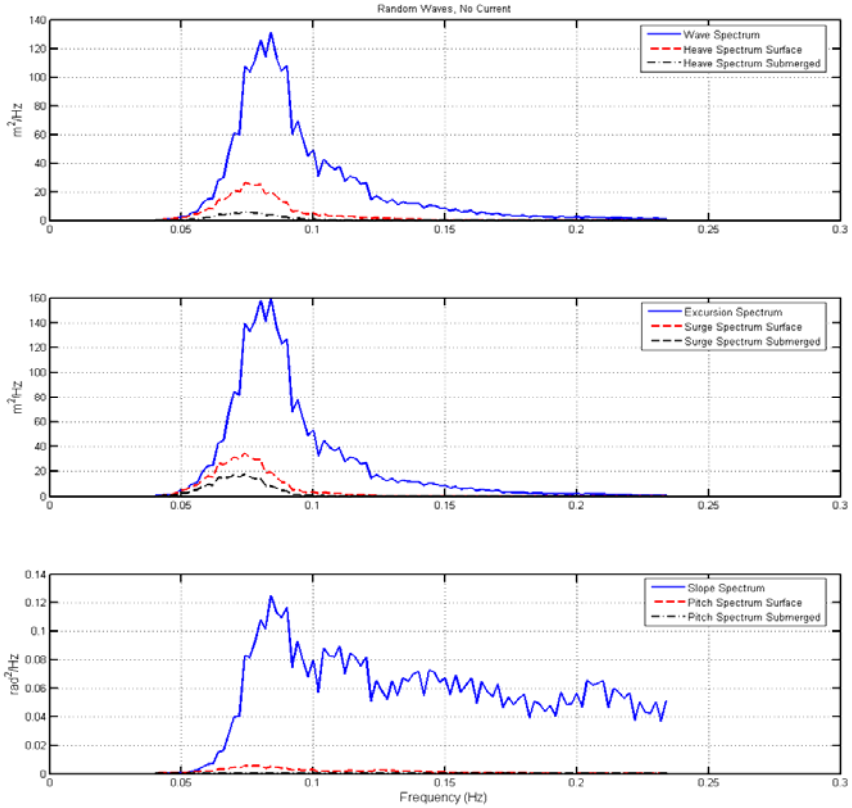

Figure 9: Motion spectral results of the random wave simulations without current.

The wave parameter input and the fish cage motion response spectra were used with equations (12), (13) and (14) to obtain the heave, surge and pitch linear transfer functions, respectively. The motion transfer function plots are indicated in Fig. 10.

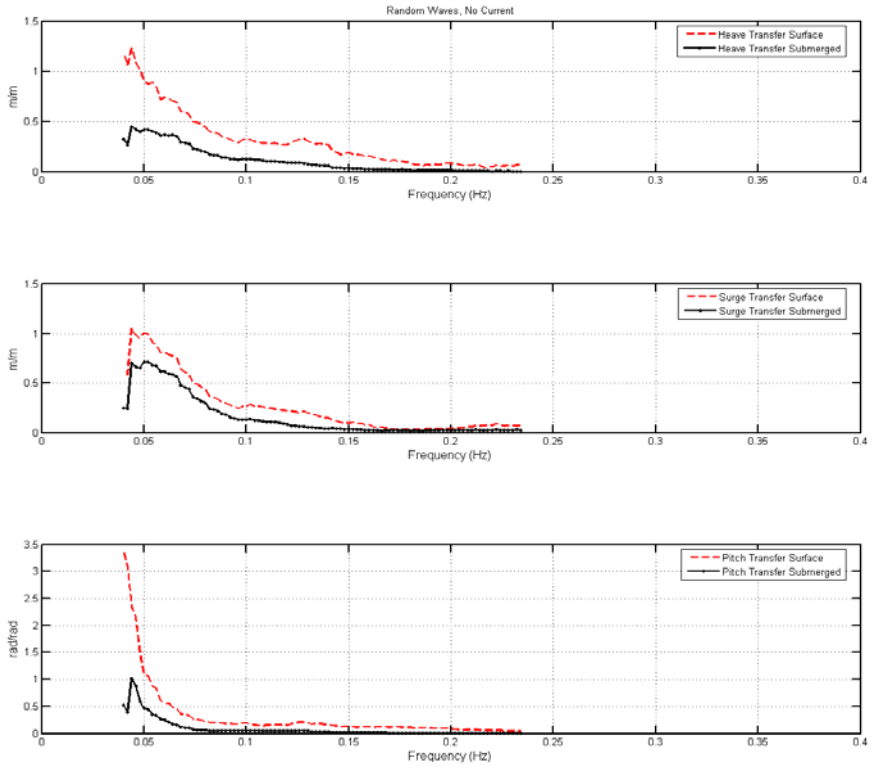

Figure 10: Motion transfer function results of the random wave simulations without current.

In addition to the transfer function calculations, the motion response was characterized by the zeroth moment of each spectral response using equations (7) and (8). The result for equation (8) calculation, called the significant response, is indicated in Tab. 7.

Table 7: Significant motion response of the submersible fish cage system

Configuration	Heave (m)	Surge (m)	Pitch (rad)
Surface	3.4670	3.8686	0.0707
Submerged	1.5512	2.6817	0.0192

Conclusion:

A numerical model was used to obtain the motion responses of a Korean automatic submersible fish cage system. We conducted simulations of the system using a Morison equation type model. The first set of tests conducted with the fish cage system was performed with no force to verify the static characteristics of the system. The next set of tests was performed with the numerical

model in regular and irregular waves (JONSWAP spectrum) with and without the 1.0 m/s current. Heave, surge and pitch dynamic calculations were made. In all simulations of a submerged cage subjected to currents for the design of a full-scale system, countermeasures considering the buoyancy increase of upper floats were needed to protect the front lower rim of the cage as it touched the seafloor. The pitch motion was prominent for surface and submerged conditions. The heave motions submerged below 20 m of the mean water level were 52.35% to 86.02% smaller than those at the surface condition. Further verifications by physical model tests and in-situ measurements including the mooring tension are needed to analyze the hydrodynamics characteristics of the cage system more accurately.

Acknowledgements:

This research was supported by Technology Development Program for Fisheries, Ministry for Food, Agriculture, Forestry and Fisheries, Republic of Korea.

References:

✓ DeCew J., Fredriksson, D.W., Bougrov, L., Swift, M.R., Eroshkin, O. and Celikkol, B. (2005) Numerical and physical modeling of a modified gravity type cage and modeling system. IEEE J. of Ocean. Eng. 30(1), 47-58.

✓ Fredriksson, D.W., Swift, M.R., Irish, J.D., Tsukrov, I. and Celikkol, B. (2003a) Fish cage and mooring system dynamics using physical and numerical models with field measurements. Aqua. Eng. 27(2), 117-270.

✓ DeCew J., Fredriksson, D.W., Bougrov, L., Swift, M.R., Eroshkin, O. and Celikkol, B. (2005) Numerical and physical modeling of a modified gravity type cage and modeling system. IEEE J. of Ocean. Eng. 30(1), 47-58.

✓ Fredriksson, D.W., Swift, M.R., Irish, J.D., and Celikkol, B. (2003b) The heave response of a central spar fish cage. Transactions of the ASME. J. of Off. Mech. and Arct. Eng. 25, 242- 248.

✓ Haritos, N and He, D.T. (1992) Modelling the response of cable elements in an ocean environment. Fin. Elem. In Analysis and Des. 19, 19-32.

✓ Hasselmann, K. (1973) Measurements of wind-wave growth and swell decay during the Joint North Sea Wave Project (JONSWAP). Deutsche Hydrographische Zeitschrift. Reihe, 12.

✓ Kim, T.H. (2006) Mooring loads analysis of submersible aquaculture cage system using finite element method. J. Kor. Soc. Fish. Tech. 42(1), 44-53.

✓ Kim, T.H., Fredriksson, D.W. and Decew, J. (2008) Hydrodynamics of submersible aquaculture cage system using numerical model. J. Kor. Soc. Fish. Tech. 44(1), 46-56.

✓ Kim, T.H., Yang, K.U., Jang, D.J. and Fredriksson D.W. (2010a) The submerging characteristics of a submersible fish cage system operated by compressed air. MTS J. 44(1), 57-68.

✓ Kim, T.H., Yang, K.U., Hwang, K.S., Jang, D.J. and Hur, J. G. (2010b) Automatic surfacing and submerging performances of model fish cage system operated by air control. JWAS. (in submitted).

✓ Mitrovich, V. (2010) The wait is over. Fish Farming International. 37(2), 20-24.

- ✓ Morison, J. R., Johnson, J.W., O'Brien, M.P. and Schaaf, S.A. (1950) The forces exerted by surface waves on piles. Petroleum Transactions. American Inst. Of Mining Eng. 149-157.
- ✓ Ochi, M.K. (1998) Ocean Waves: The Stochastic Approach. Cambridge University Press, New York.
- ✓ Shore Protection Manual (1984) 4th ed., 2 Vols., US Army Engineer Waterways Experiment Station, Coastal Engineering Research Center, US Government Printing Office, Washington, DC.
- ✓ Tsukrov, I., Eroshkin, O., Fredriksson, D.W., Swift, M.R. and Celikkol, B. (2003) Finite element modeling of net panels using consistent net elements. Ocean Eng. 30, 251-270.
- ✓ Tsukrov, I., Eroshkin, O., Paul, W. and Celikkol, B. (2005) Numerical modeling of nonlinear elastic components of mooring systems. IEEE J. Oceanic. Eng. 30(1), 37-46.